The Redox Properties of Cytochromes *b* Imposed by the Membrane Electrostatic Environment

Lev I. Krishtalik,* Gun-Sik Tae,‡ Dimitri A. Cherepanov,* and William A. Cramer‡§

‡Department of Biological Sciences, Purdue University, West Lafayette, IN 47907 USA; *Frumkin Institute of Electrochemistry, Academy of Sciences, Moscow 117 071, Russia

ABSTRACT The effect of the dipole potential field of extended membrane spanning α-helices on the redox potentials of *b* cytochromes in energy transducing membranes has been calculated in the context of a three phase model for the membrane. In this model, the membrane contains three dielectric layers; (i) a 40-Å hydrophobic membrane bilayer, with dielectric constant $\epsilon_m = 3–4$, (ii) 10–20-Å interfacial layers of intermediate polarity, $\epsilon_{in} = 12–20$, that consist of lipid polar head groups and peripheral protein segments, and (iii) an external infinite water medium, $\epsilon_w = 80$. The unusually positive midpoint potential, $E_m = +0.4$ V, of the "high potential" cytochrome *b*-559 of oxygenic photosynthetic membranes, a previously enigmatic property of this cytochrome, can be explained by (i) the position of the heme in the positive dipole potential region near the NH_2 termini of the two parallel helices that provide its histidine ligands, and (ii) the loss of solvation energy of the heme ion due to the low dielectric constant of its surroundings, leading to an estimate of +0.31 to +0.37 V for the cytochrome E_m. The known tendency of this cytochrome to undergo a large $-\Delta E_m$ shift upon exposure of thylakoid membranes to proteases or damaging treatments is explained by disruption of the intermediate polarity (ϵ_{in}) surface dielectric layer and the resulting contact of the heme with the external water medium.

Application of this model to the two hemes (b_n and b_p) of cytochrome *b* of the cytochrome bc_1 complex, with the two hemes placed symmetrically in the low dielectric (ϵ_m) membrane bilayer, results in E_m values of hemes b_n and b_p that are, respectively, somewhat too negative (approximately −0.1 V), and much too positive (approximately +0.3 V), leading to a potential difference, $E_m(b_p) - E_m(b_n)$, with the wrong sign and magnitude, +0.25 V instead of −0.10 to −0.15 V. The heme potentials can only be approximately reconciled with experiment, if it is assumed that the two hemes are in different dielectric environments, with that of heme b_p being more polar.

INTRODUCTION

The pigmented proteins of energy-transducing membranes are excellent models for analysis of structure-function relationships of membrane proteins, because they can be analyzed not only by the molecular biological, biochemical, and structural approaches that can be applied to all membrane proteins, but also by the quantitative tools of spectroscopy and electrochemistry.

The nature of parameters that govern the effective redox potentials of prosthetic groups in soluble or membrane-attached proteins has been discussed extensively (1–7). A fundamental parameter that has not previously been considered in discussions of oxidation-reduction properties of membrane-bound heme proteins is that of the electric field arising from the *trans*-membrane α-helices that are known to be fundamental in the structure of membrane proteins (8).

A substantial electrostatic field can exist in proteins that significantly affects the thermodynamics and kinetics of enzymatic reactions (9–15). The secondary structure of intrinsic membrane proteins that creates the strong field is the α-helix which presents a system of practically parallel dipole moments of peptide groups (16, 17), and which is substantially longer on the average in *trans*-membrane helices than in soluble proteins (18).

The effect of the dipole field arising from *trans*-membrane α-helices is considered in the present work for (i) the cytochrome *b*-559 of the photosystem II (PSII)[1] reaction center of oxygenic photosynthesis (19), and (ii) cytochrome *b* of the bc_1 complex that connects the reducing and oxidizing ends of the electron transport chains in mitochondria and photosynthetic bacteria (bc_1) (7). The aspect of the structure of these integral membrane-bound cytochromes that makes it possible to consider the redox potentials in a relatively simple dielectric model is that (*a*) their dominant structural motif is the *trans*-membrane α-helix; (*b*) cytochrome *b*-559 and cytochrome *b* of the bc_1 complex are "ideal" integral membrane proteins because the *trans*-membrane helices of the heme-binding domain do not contain any charged basic (Arg, Lys) or acidic (Glu, Asp) amino acids (20).

The presence of cytochrome *b*-559 in the PSII reaction center as a heme-bridged heterodimer with the heme near the stromal edge of the membrane bilayer (21) constitutes a major structural difference between this reaction center and that

Received for publication 26 May 1992 and in final form 1 March 1993.

Address reprint requests to W. A. Cramer.

§ To whom correspondence should be addressed. Tel.: 317-494-4956; fax: 317-494-0876.

0006-3495/93/07/184/12 $2.00

[1] *Abbreviations used in this paper:* PSII, photosystem II; cyt, cytochrome; D, debye unit; D1,D2, polypeptides of the photosystem II reaction center, containing 344 and 353 residues, respectively, in spinach chloroplasts; E_m, midpoint potential; heme b_n, b_p, hemes on the electrochemically negative and positive sides of the membrane, respectively; HP, LP, high, low redox potential; LHC, light-harvesting chlorophyll protein; PSII, photosystem II, sodium dodecyl sulfate polyacrylamide gel electrophoresis; TBS, Tris-buffered saline.

of the photosynthetic bacteria (8). This cytochrome has an unusually positive (+0.4V) midpoint potential (22).

It is known that the high potential (HP) state of this cytochrome is correlated with the freshness and intactness of the membrane preparations used for its assay, and that the HP state (E_m = +0.4 V) is converted to a low potential (LP) state with E_m = +0.05–0.1 V when the membranes are aged or damaged. The physicochemical basis for the unique HP state and the HP → LP conversion associated with membrane damage has not been provided and is a long-standing problem in studies on photosynthetic electron transport and photosystem II (23). The present study can provide an explanation for these electrochemical properties of the cytochrome *b*-559 in the context of a three phase dielectric model, with a hydrophobic niche for the cytochrome heme, and a protective surface proteinaceous layer of intermediate dielectric constant that protects this niche from the bulk external high dielectric H_2O.

The use of the three phase model to describe the E_m values of the two hemes b_n and b_p located on opposite sides of the membrane of the cytochrome *b* of the bc_1 complex did not yield qualitatively reasonable values compared to experiment, unless it was assumed that heme b_p occupies a more polar dielectric environment than heme b_n.

METHODS AND RESULTS

The calculation of the electric field of an α-helix in membranes must take into account the interaction of partial charges of atoms with polar surroundings adjacent to the hydrocarbon inner layer of the membrane. This interaction is usually described as a superposition of a direct Coulombic field of a given atom with the fields of its "images" situated in other dielectric phases (13, 24, 25).

A model of the biological membrane has been developed (Fig. 1 *A*) which takes into account the important feature of the membrane as a multilayer structure (26). In this model, the low dielectric (ϵ_m) hydrocarbon layer of approximately 40-Å thickness is bordered by two layers with intermediate polarity and dielectric constant (ϵ_{in}). The latter layers correspond to the region of lipid polar head groups (approximately 10-Å thick [27]) and extrinsic segments of membrane proteins containing hydrophilic or charged side chains and water. The high content of water inside extrinsic proteins of the bacterial photosynthetic reaction center is documented by x-ray structure analysis (8). Because these water molecules are visible by x-ray diffraction, their mobility and their contribution to the effective dielectric constant are lower than in bulk water. The adjacent bulk aqueous solution has a dielectric constant, ϵ_w = 80. However, because of the presence of electrolytes in the solution that will screen the field more strongly, resulting in a situation where the Debye screening length was shorter than the distance to the nearest image, a quasimetal approximation with $\epsilon_w = \infty$ was used (28).

In calculations involving the dielectric constant of the hydrophobic membrane region, values of ϵ_m = 3 or 4 were used. The latter value is typical of the interior of globular proteins (see, e.g., Refs. 5, 10, 11, 13, and 15) and reflects the emphasis in this work on the behavior of hemes immersed in the interior of large membrane protein complexes. ϵ_m = 3 was also used as the average of ϵ_m = 2 for the lipid hydrocarbon region and ϵ_m = 4 for protein interiors. The dielectric constant, ϵ_{in}, of the lipid polar-head region is in the range 12–20. This estimate is based mainly on the electrical response of biological and model bilayer membranes (26, 29–31). The thickness of this interlayer was assumed to be 10 Å. The results of calculations were practically insensitive to variation in the thickness of the ϵ_{in} interlayer from 8 to 20 Å.

To calculate the electric field, it is necessary to know the partial charges of atoms in the peptide group. The charges corresponding to a dipole moment of the peptide bond ≈4 D have often been reported (e.g., Refs. 17 and 32). This is the dipole moment of free amide molecules, and practically the same values result from quantum-chemical calculations for amides and di- or tripeptides. However, this value appears to underestimate the dipole moment of the peptide bond. Direct measurement of the dipole moment/residue in a homogeneous helical polypeptide indicated a value ≥ 6 D (33). Comparison of structural data for amides and proteins shows that in proteins the C′-N distance is shorter by 0.04–0.05 Å and the C′-O distance longer by 0.03–0.05 Å than in amides. This points to an increased double bond character of the C′-N bond and an opposite tendency for the C′-O bond, which thereby results in an increased contribution of N^+ and O^- states, and hence, an increased dipole moment (34). Finally, quantum-chemical calculations

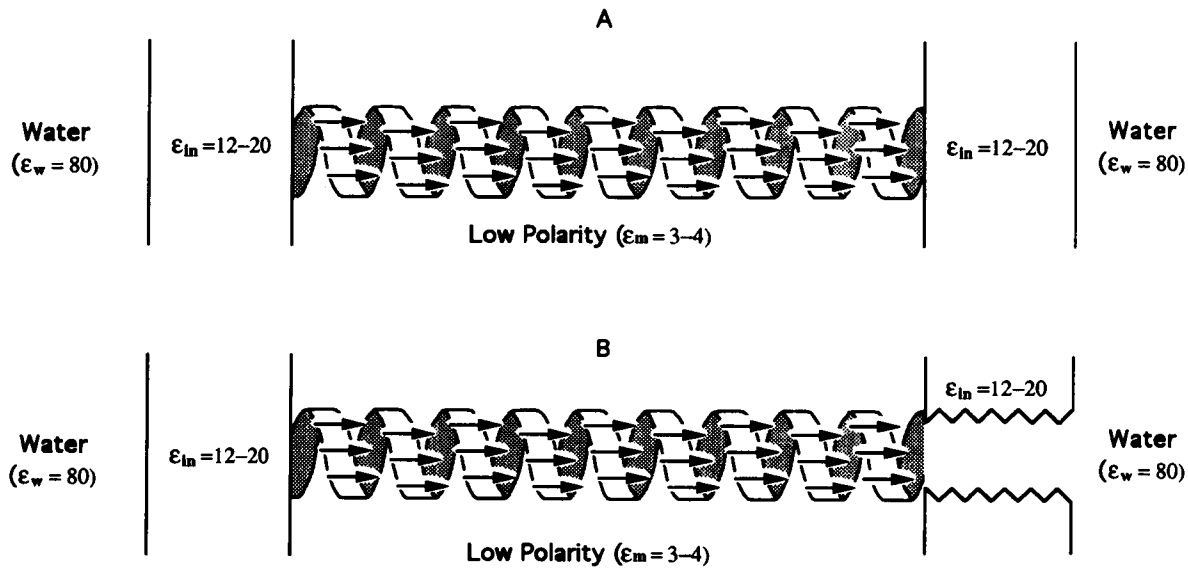

FIGURE 1 (*A*) Schematic three dielectric layer model of a hydrophobic membrane-spanning α-helix inserted into a membrane of low (ϵ_m = 3–4) dielectric constant that is bounded by 10–20-Å layers of intermediate (ϵ_{in} = 12–20) polarity. The aligned dipoles of the peptide groups are shown, with the NH_2 and COOH termini of the helix on the right and left, respectively. (*B*) Schematic of three layer model with layer of intermediate polarity disrupted on side near NH_2 terminus of helix, mimicking a disruption on stromal side of thylakoid membrane that causes negatively directed E_m shift.

for larger peptides have shown that starting from a tetrapeptide, i.e., from a helical configuration in which the peptide group can form hydrogen bonds, the average dipole moment of each group increases substantially, exceeding 5 D and approaching 6 D. This effect is caused by the mutual polarization of the hydrogen-bonded groups (35). In the present calculations, the following approximate values for the partial charges, which yielded a dipole moment of 5.9 D, were used: C, +0.7; O, −0.7; N, −0.4; H, +0.4.

The electric field near the α-helix surface reflects the helical symmetry and changes with distance from the helix axis in a somewhat complicated way (26). At distances from the helix axis >7 Å, this dependence is smoother (Fig. 2, *A* and *B*). The value of the potential can be seen to decrease with distance from the helix axis (e.g., 7 (○) and 9 (□) Å, Fig. 2 *A*). Some deviation from true cylindrical symmetry, arising from the influence of details of the helical structure, may be seen in these curves, i.e., the positive potentials are somewhat higher in absolute value than the negative ones. For the dependence along the normal to the membrane plane situated on the other side of the helix axis, the situation is reversed. The potentials are larger, the further the helix termini from the membrane boundary, i.e., the less the screening of the field by the more polar dielectric in the ϵ_{in} layers (e.g., 3 (□) and 1 (○) Å from boundary, Fig. 2 *B*). This screening effect also explains the larger asymmetry of the potential distribution for helices tilted from the normal to the membrane surface (Fig. 2 *A*).

Besides the intraprotein electric field, an important factor affecting the heme redox potential is the loss of the electrostatic (Bornian) solvation

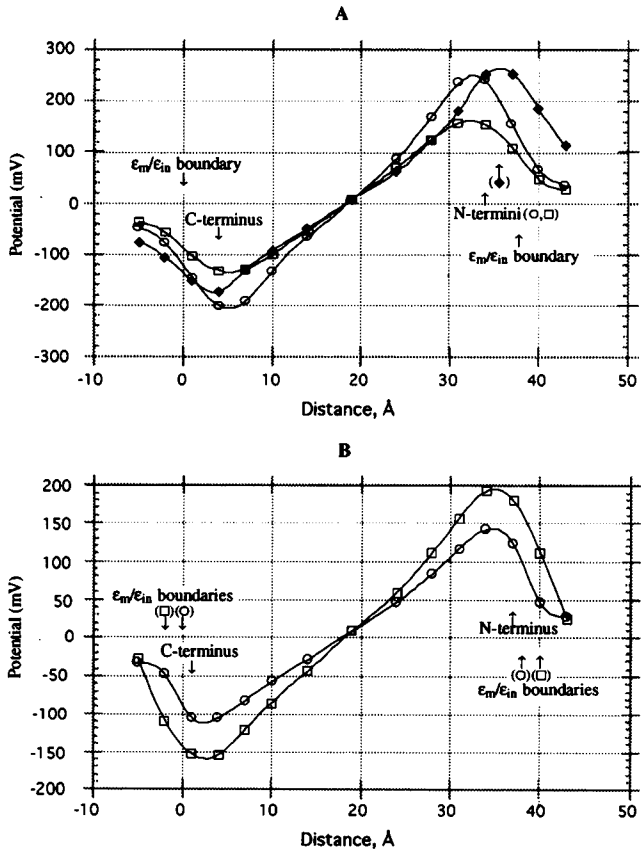

FIGURE 2 Potential distribution parallel to the helix axis in the plane where the first C_α from the COOH terminus is situated. (*A*) 20-residue α-helix with C-terminal C_α atoms at a distance of 4 Å from the dielectric boundary with the intermediate polarity (ϵ_{in} = 12–20) phase; thickness of low dielectric bilayer, 38 Å; distance from helix axis 7 (○) and 9 Å (□). Also shown is the potential distribution 7 Å from the axis of a 24-residue helix tilted 30° to the normal, with the COOH-terminal C_α atom 4 Å from the boundary (◆). (*B*) 24-residue α-helix, 8 Å from helix axis; distance of COOH-terminal C_α from dielectric boundary, 1 (○) and 3 Å (□), with the thickness of the low dielectric bilayer 38 and 42 Å, respectively.

energy due to the transfer of an ion from water (dielectric ϵ_w) into the low dielectric membrane bilayer (ϵ_m). For the infinite uniform dielectric, the last component is described by

$$\Delta G_{Born} = \frac{(Ze)^2}{2a}\left(\frac{1}{\epsilon_m} - \frac{1}{\epsilon_w}\right) \quad (1)$$

where *Ze* is the charge and a is the radius of the spherical ion.

For the radius of a large complex ion, one can use the radius of a sphere enclosing the van der Waal's envelope including all ligands. Such an approximation in the case of large (a ≥ 4 Å) ions describes ion transfer energies with an accuracy ≤10 mV (36, 37). In the present case, the iron ligands are the four heme nitrogen and two histidine imidazole rings. These ligands are assumed to be only heme and imidazole with all side groups replaced by hydrogen. The average radius of the van der Waal's envelope of this roughly spherical complex was estimated to be 6.5 Å. Calculations according to Eq. 1 with ϵ_m = 4 give ΔG_B = 263 meV. The upper and lower limits of this value were obtained by: (i) substituting methyl and vinyl chains to the heme and a methyl group for the linkage of imidazole to the helix backbone which yielded a radius of approximately 8.0 Å; (ii) a lower limit of 5.5 Å was obtained by discarding all hydrogen atoms. The corresponding values of ΔG_B, which are believed to be conservative limits, are 214 and 311 meV, respectively. It is concluded that for ϵ_m = 4, ΔG_B = 0.26 eV is a reasonable estimate with an accuracy better than 0.05 V. For the lower ϵ_m value equal to 3, ΔG_B = 0.35 eV (see below, calculations for cyt *b*-559; Table 1).

In a nonuniform dielectric system corresponding to a real membrane (e.g., Fig. 1 *A*), the total charging energy equals the Bornian energy (Eq. 1) plus a term from the image charges. The image force contribution equals $e\varphi_{im}/2$, where φ_{im} is the potential created by all the images of the real charge *Ze* at its center. This contribution has a sign opposite to ΔG_B, because the principal images in more polar media have a sign opposite to that of *Ze*. Hence, the total loss of solvation energy is less than ΔG_B.

Calculations of the midpoint redox potential of cytochrome b-559

A molecular model of the *trans*-membrane α and β helices of the chloroplast PSII cytochrome *b*-559 was constructed using the program FRODO on an Evans-Sutherland PS300 computer (Fig. 3). Both $N_{\epsilon 2}$ of His^{22} (α subunit) and His^{17} (β subunit) of the two α-helices were placed on the common perpendicular to the heme plane crossing it at the center (iron center), with the Fe-N distances at 1.82 and 1.85 Å. This geometry is similar to that observed experimentally for cyt b_5 (38), where the two Fe-N distances are 1.90 and 1.78 Å, and their average (1.84 Å) is close to those used for cyt *b*-559. The two His C_α atoms in the *b*-559 model were placed symmetrically on the same perpendicular, because steric restrictions of two parallel helices prevent tilt of the C_α-N_ϵ line relative to the heme plane observed in cyt b_5. The *b*-559 model was checked for the absence of interhelix contacts closer than the sum of van der Waal's radii. The distance from the helix axis of the heme iron, the center of positive charge in the oxidized heme, was determined to be 8.7 Å. This value is practically the same for both helices.

To describe the position of the heme iron atom along the axis of the α-helix (*z*-axis), the origin (z = 0) has been defined to be at the position of the first α-carbon. This choice is independent of the distance between the end of the helix and the ϵ_m/ϵ_{in} boundary. The ϵ_m/ϵ_{in} boundary was used as the origin for the graph of the potential distribution along the helix axis in Fig. 2 *A* and in Fig. 2 *B* for the case of a 1-Å separation between the boundary and the COOH-terminal α-carbon. The *z* coordinate at the iron position is 7.5 Å, assuming that both His are fifth residues from the interface with the His C_α on the perpendicular crossing the heme Fe. The calculations of the electric potential of the α-helix 7 and 9 Å from the helix axis (Fig. 2 *A*, (○) and (□), respectively) show that the dependence of the potential on distance along this perpendicular changes slowly with distance, so an error of the order of 0.5 Å would result in a potential shift of <10 mV. The potential depends slightly on the rotation angle in cylindrical coordinates (zero value corresponding to position of first α-carbon) around the helix axis (data not shown). In the calculation for the potential at the position of the heme, the appropriate angle was derived from the structural model shown in Fig. 3.

TABLE 1 Components of the midpoint redox potential (E_m) of cytochrome *b*-559

A. Potential in aqueous solution (volts)		−0.15	
Distance, δz, Å, between first C_α atom and ϵ_m/ϵ_{in} boundary	−1	+1	+3
Shift of potential (volts) due to:			
B. Bornian solvation energy	+0.25	+0.27	+0.28
C. Interaction with the field of two α-helices	+0.19	+0.19	+0.24
Value of midpoint redox potential, E_m(volts) Experimental value = +0.40V	+0.29[a]	+0.31	+0.37

[a] This value was considered less likely; see Methods.

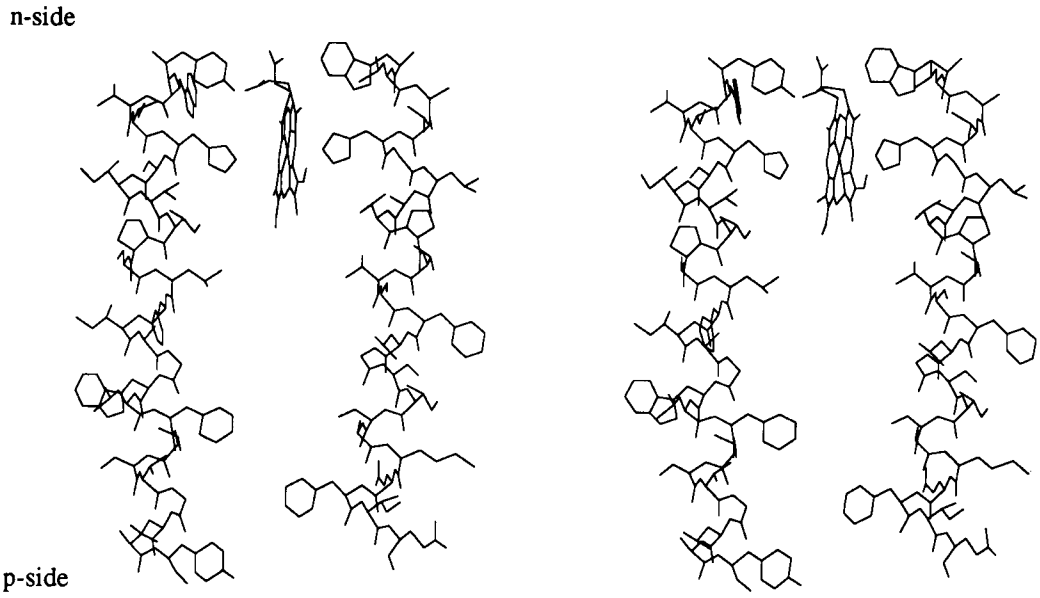

FIGURE 3 Molecular model (*stereo view*) of cytochrome *b*-559 showing the heme bridged α (*left*) and β (*right*) helices. The amino acid sequences of these helices are (with *trans*-membrane helical segments *underlined*): (α) NH_2 (*top*)-SGSTGERSFADIITSIRYWVIHSITIPSLFIAGWLFVSTG LAYDVFGSPRPNEYFTESRQGIPLITGRFDSLEQLDEFSRSF-COOH; (β) NH_2 (*top*)-TIDRTYPIFTVRWLAIHGLAVPTVSFLGSISAMQFIQR-COOH. Stromal (*n*) side of the membrane (*top*); lumen (*p*) side (*bottom*).

Due to the fact that the region of interest in the bilayer is situated rather far from the boundary, the effect of ϵ_{in} on the calculated potential was small. The potential for $\epsilon_{in} = 12$ given in Table 1 exceeded that at $\epsilon_{in} = 20$ by ~10 mV, and the difference in Bornian energies does not exceed 3 meV.

These calculations provide the shift of the heme potential in the membrane relative to its value in aqueous solution. The absolute value of the heme *b* potential in water requires some discussion. The value of $E_m \geq +0.08$ V refers to a pH-dependent potential (1). This dependence may be ascribed to ligand substitution: OH^- for imidazole (1, 39) or acid dissociation of bound imidazole (40). However, at physiological pH, the above ligand changes are not likely. Hence, one needs as a reference the potential in aqueous solution of the pure electron transfer reaction without any chemical transformation in the inner coordination sphere of the iron. The basis for the estimate of this potential as $E = -0.1$ V (39) is not clear, because the paper referenced (41) does not contain data on the E_m behavior in a pH-independent region. Such data were obtained by Warme and Hager (40) for *bis*-histidine mesoheme. Taking into account the 70-mV shift of the potential of protoheme relative to mesoheme (1), the reference potential is estimated to be $E_m \approx -0.15$ V (Table 1 *A*). The main energetic components affecting the midpoint redox potential of cytochrome *b*-559 are summarized in Table 1, *A–C*.

It is probable that the cyt *b*-559 heme is not totally surrounded by protein α-helices, but also by lipid hydrocarbon chains that are adjacent to the heme. This is implied by the ability of lipophilic anionic charge carriers to catalyze the oxidation of the cytochrome (42). Hence, it is reasonable to use an average ϵ_m value intermediate between $\epsilon_m = 4$ typical of protein and $\epsilon_m = 2$ characteristic of hydrocarbons. The data given in Table 1 are calculated with $\epsilon_m = 3$. For $\epsilon_m = 4$, the Bornian energy loss (Table 1 *B*) is smaller by 0.08 eV, the field effect lower by 0.04 eV, and the net E_m less positive by 0.12 eV.

The results shown in Table 1 are not very sensitive to small variations in (i) the value of ϵ_{in}, or (ii) the distance between the helix C_α atom and the ϵ_m/ϵ_{in} boundary. Variation of $\Delta(\delta z)$ by −2 or +2 about the value $\delta z = +1$ results in a correction of −0.02 or +0.06 V, the former value corresponding to protrusion of the α-helices from the hydrophobic domain of the membrane. This alternative appears to be less probable, because in this case it would be difficult to explain the experimental fact of inaccessibility of arginine 17 (Arg^{17}, Fig. 3) of the α subunit to protease (21). Therefore, from these considerations, the E_m of cyt *b*-559 is calculated to be 0.31–0.37 V depending on the distance of the heme from the layer of intermediate polarity, ϵ_{in}. This calculation is considered to be a first approximation, and several other interactions should be kept in mind. Besides the effects listed in Table 1, *A–C*, other factors can be recognized that could influence the potential: (i) the tilt of the cyt *b*-559 helices; the fields of (ii) the ionized heme propionate groups, (iii) charged lipid head groups, (iv) the positively charged Arg^{17} at the NH_2 terminus of the α-helix, (v) a noncoplanar orientation of the imidazole ligands, and (vi) the helices of the proteins that are neighbors of cyt *b*-559 in the PSII reaction center.

(i) In the model of Fig. 3, the α and β helices of cyt *b*-559 were assumed to be parallel. However, they are bridged only at one residue, and hence could be oriented at some small angle caused by electrostatic repulsion of parallel dipoles. This angle cannot be too large to preserve an intramembrane position of hydrophobic helices and protrusion of the charged residues at the helix termini into a more polar region. Calculation of the field arising from

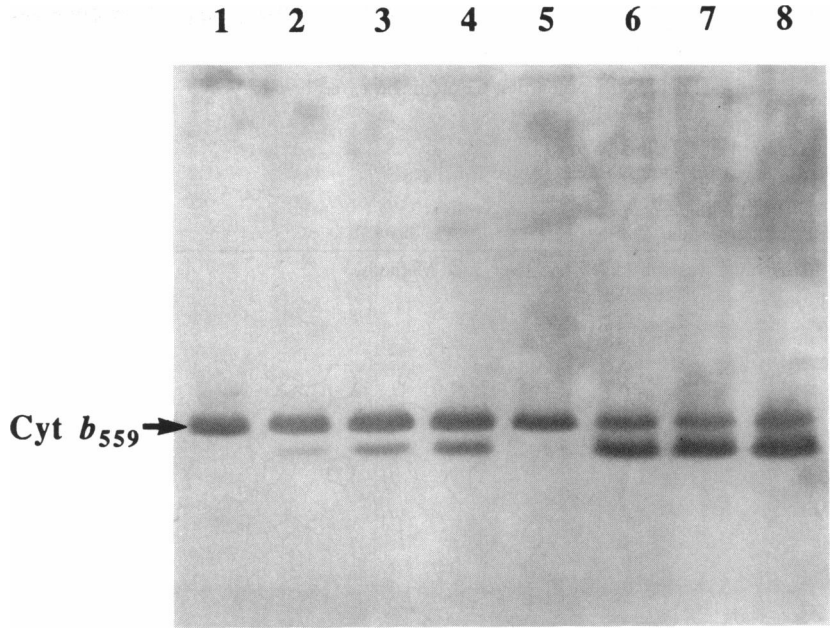

FIGURE 4 Effect of the heat treatment on accessibility of the NH_2-terminal domain of the cytochrome *b*-559 α-subunit to trypsin. Intact (lanes *1–4*) and heat-treated (lanes *5–8*) thylakoid membranes were proteolyzed (trypsin:chlorophyll, 1:50) for 0 (lanes *1* and *5*), 5 (lanes *2* and *6*), 10 (lanes *3* and *7*), and 15 min (lanes *4* and *8*). Each lane of the 15–20% gradient SDS-gel including 4 M urea was loaded with the membrane equivalent of 10 μg of chlorophyll. The gel was incubated in 10 mM Tris-HCl, pH 8.0, including 17 mM boric acid and 2 mM SDS (10 min, 25°C) and transferred to a nitrocellulose filter (Hybond-C) using a Hoefer TE 70 semi-dry transfer blotter (130 mA, constant current, 30 min). Color reactions were performed with 0.017% 4-chloro-1-naphthol and 0.05% H_2O_2 in Tris-buffered saline.

a 20-residue helix tilted at 30° to the normal (not shown in Fig. 2) indicates that the total field at the heme iron would increase by 0.07–0.1 V.

(ii) Considering the ionization state of the heme propionates, for δz = +1 Å, the center of the heme is positioned at a distance of 8.5 Å from the boundary. That means that the center of the carboxylate of the heme propionates is inside the low polarity region and cannot approach closer than 0.5 Å to the boundary. At this position, its Bornian energy loss can be estimated as approximately 0.2–0.3 eV.[2] Taking into account the positive field of α-helices at this position, approximately 0.1 V, partly compensating the solvation energy loss, one may expect proton dissociation in this carboxylate at physiological pH values. For the second carboxylate, the dissociation is much less probable due to strong electrostatic repulsion from the first CO_2^- causing an energy loss on the order of ≥0.2 eV and an additional $\Delta pK \geq 3$. The anion at the position of the propionates would shift the heme redox potential by −0.1 V, but this value must be compared with the corresponding shift in aqueous solution due to the action of two CO_2^- ions. The latter is approximately 0.05 V, so the total negative shift relative to the potential in water is −0.05 V.[3]

(iii) Anionic lipid head groups are situated outside the low dielectric bilayer containing the bundle of parallel α-helices. They are then far from the hemes and closer to the water interface, leading to a small or negligible contribution to the heme E_m.

(iv) A small positive shift due to the field of two guanidinium ions of arginines (α Arg^{17}, β Arg^{12}) situated in the polar-head region is expected. If they approach the boundary at a distance of 2 Å, the van der Waal's radius of the NH group and hence the distance of closest approach to the low-polarity phase, then the total effect of these ions may be estimated, depending on their position along the boundary, as 0.05–0.1 V. In general, the total effect of all ions does not exceed ±0.05 V.

(v) A noncoplanar orientation of the histidine ligands was inferred from EPR spectra (3). This effect might also cause a small positive shift (≤ +0.05V) of the E_m (47).

The net effect from the additional smaller effects discussed in (i-v) above would be to shift the E_m value to a somewhat more positive (approximately 0.1 V) value with an uncertainty of approximately ±0.1 V.

(vi) It is impossible to calculate a better approximation and to accurately take into account the interaction of any other *trans*-membrane helices from the major "D1" and "D2" polypeptides that are in the PSII reaction center complex without additional structure information about the complex. The "D1" and "D2" polypeptides each span the bilayer five times. However, the above first approximation involving isolated cyt *b*-559 in the membrane may be reasonably accurate, because interaction of the cytochrome with the other PSII polypeptides is inferred not to be strong from the following data: (*a*) there is no fast electron transfer between the cyt *b*-559 heme and the redox centers on the oxidizing side of PSII (48). (*b*) In fact, the only electron transfer reactions of the cytochrome of significant amplitude that can be observed require the presence of lipophilic molecules such as quinones (23) or lipid-soluble anions (42); (*c*) cytochrome *b*-559 can be separated with nonionic detergent from the reaction center, leaving a photoactive D1-D2 core (49). These data suggest that cyt *b*-559 may be separated from the D1-D2 polypeptides by boundary lipid. The first approximation for the calculation of the E_m value of cyt *b*-559 appears reasonable on this basis.

[2] In this estimate, the charging energy for the ion crossing the boundary was calculated according to the scheme proposed by Kharkats and Ulstrup (43).

[3] The electrostatic effect of propionate anion on E_m of cytochromes has been discussed (4, 44–46). Quantitative electrostatic calculation for cyt c_{551} gives the potential shift of −0.09V in reasonable agreement with the experimental estimate ΔE_m = −0.065V (46). This effect is close to the estimate for intramembrane cyt *b*-559 given above. A detailed analysis of electrostatics for the reaction center cyt *c* was given recently by Gunner and Honig (6). Their estimate for this effect gives much larger values (up to ~−0.3 V), when the anion is buried deeply in the protein. On the contrary, in the system described in the present work, the negative charge is situated rather close to the region of higher polarity, and hence its electric field is substantially screened.

Experimental treatments affecting the E_m of cyt b-559

Trypsinization of the thylakoid membrane surface, including cleavage of a seven-residue N-terminal peptide from the α subunit of cyt *b*-559 (21), shifts the redox potential by 0.2–0.3 V in the negative direction, i.e., from +0.395 V to an E_m where it is not reducible by an excess of hydroquinone (E_{m7} = +0.26 V [50]). The E_m may be as negative as its low potential form [E_{m7} = +80 mV] [51]. Light-harvesting chlorophyll protein (LHC) polypeptides associated with PSII are very sensitive to trypsin, as is the D1 and other PSII proteins (50). Other damaging treatments such as heat also cause a large negatively directed shift in the E_m of cyt *b*-559 (52). The effect

of heat treatment in causing an increase in the accessibility of H_2O to the membrane surface, monitored by the effect of the water-soluble protease, trypsin, on the cyt *b*-559 α subunit near the stromal membrane surface, is shown by the time course of protease action measured by the technique of sodium dodecyl sulfate-polyacrylamide gel electrophoresis (Fig. 4). Trypsin causes proteolysis of the cyt *b*-559 α subunit after the residue Arg[7]. In control membranes, the proteolysis is indicated by the appearance of a slightly smaller (ΔM_r = –800) band, whose amount increases as the time of incubation with a trypsin is increased from 5 to 15 min (Fig. 4, lanes *2–4*). After heat treatment (50°, 5 min), the proteolysis reaches its maximum extent within a 5-min incubation time with trypsin (lanes *6–8*, Fig. 4).

To simulate the effect of this kind of disruptive treatment, it was hypothesized that the cyt *b*-559 surface hydrophilic peptide and surface segments from the LHC, D1, and D2 reaction center polypeptides form a polar cap on the membrane with a dielectric constant ϵ_{in} (Fig. 1 *A*) that screens the NH_2 termini of the cytochrome α-helices from the bulk water phase. Proteolytic cleavage of this surface-bound proteinaceous domain by trypsin would damage the surface protective layer and bring the low dielectric (ϵ_m) layer in direct contact with water. This effect was calculated in the framework of the model shown in Fig. 1 *B* in which the intermediate polarity surface layer on the outside stromal surface is removed, and the low polarity region (ϵ_m = 3–4) of the membrane becomes directly adjacent to water without any interlayer. The consequence is (i) a stronger interaction of the charged heme with water and (ii) more effective screening of the α-helix electrical field by the aqueous solution. Both effects decrease the E_m by 0.10–0.13 V, with a total ΔE_m = –0.20 to –0.26 V, in reasonable agreement with the experimentally observed decrease in E_m value of –0.2 to –0.3 V (48).

Calculation of the E_m of the two hemes, b_p and b_n, of cyt b of the cytochrome bc_1 complex

The symmetric heme model

A structural model of the heme binding domain of cytochrome *b* of the cytochrome bc_1 complex was constructed (Fig. 5) in a manner similar to that described above for cyt *b*-559 using the sequence of the yeast mitochondrial cyt *b* (53). The heme-binding domain occupies the first four *trans*-membrane helices, the two hemes bridge helices II and IV, and the length of helices I–IV is assumed, from hydropathy analysis, to be 20, 19, 23, and 23 residues (20, 54, 55). In this case, the mutual position of helices II and IV is determined by their links via the two hemes, b_n and b_p. The planes of the hemes are positioned almost parallel to each other. Heme b_p is positioned at the fifth residue from the NH_2 terminus (6 Å along the *z* axis from the terminal C_α), and heme b_n at the fifth residue from the COOH terminus of helix IV. A similar model can be constructed for cytochrome b_6 of the b_6f complex of oxygenic photosynthesis. An important difference in the latter is that, because of the extra residue between the two histidines in helix IV of cyt b_6 (54), it is impossible to match both helices and hemes without a substantial distortion of the side chains from their optimal positions and/or a marked tilt of the imidazole rings to the heme plane.

An important property of the heme-ligating helices of these *b* cytochromes compared to those of cyt *b*-559 is that helix II is substantially shorter than helix IV, so that hemes b_n and b_p are at the third residue (3 Å) from the terminal residues of helix II in the bilayer. This results in a stronger effect of helix II on the heme E_m, because the hemes are closer to the helix termini, and the termini are further from the boundaries so that the field at the hemes is less screened. This is seen in Table 2 where the energetic components of the redox potentials of the two hemes are summarized. The model used in these calculations assumes that helix IV is positioned normal to the membrane surface and the C_α of both of its termini are 1 Å inside the low polarity phase boundary. This is a symmetric configuration with the centers of both hemes at a distance of 7 Å from the ϵ_m/ϵ_{in} boundaries. Helices I and III are also placed symmetrically relative to the boundaries and to helices II and IV. A minimal distance between the heme centers and the axes of these helices (12 Å) is assumed. For other helices, the distance from the hemes is probably much larger (see, e.g., scheme of di Rago et al. [56]), and their effect on the heme E_m is negligible.

The different results calculated for the E_m values of the *b*-559 and b_p hemes (Tables 1 and 2) near the NH_2 termini of the coordinating helices arise from: (i) contribution from the parallel helices I, III of cyt *b* (bc_1); (ii) the value of ϵ_m = 4 instead of 3 used for calculations of the cyt $b(bc_1)$ E_m values (Table 2), because its hemes are believed to be surrounded by a proteinaceous environment consisting of $\geq$10 *trans*-membrane helices of the complex.

The calculated E_m value for heme b_n (bc_1) is within 0.1–0.15 V of the experimental value of 0.05 V in chromatophores (57) or +0.09 V in mitochondria (58). For heme b_p (bc_1) the calculated result is much more positive (0.2–0.3 V) than the experimentally determined value of –0.09 V in chromatophores (57) or –0.02 V in mitochondria (58). This discrepancy exceeds any reasonable estimate of the calculation error (approximately ±0.1 V). Moreover, the calculated difference of these two potentials has the wrong sign: $E_m(b_p) - E_m(b_n) = \Delta E_m$ = +0.25 V instead of –0.10 to –0.15 V. It is not merely a quantitative discrepancy but a qualitative contradiction, which results from the positive ends of the α-helix dipoles being closer to heme b_p and the negative ends being closer to heme b_n.

There appear to be three possible structural properties of cyt *b* that might cause an additional electrostatic shift of the E_m values and eliminate the discrepancy: (*a*) the presence of an anion close to heme b_p; (*b*) a large contribution of a negative potential from the field of the short amphiphilic helix proposed to exist on the *p*-side of the membrane connecting *trans*-membrane helices III–IV (59–61), which could generate a negative potential if its COOH terminus protruded inside the low-polarity medium near heme b_p; (*c*) an asymmetric environment of the two hemes so that heme b_p is in contact with a more polar phase. At the present time, there is no information available on possibilities *a* or *b*, but there are data suggesting an asymmetric position of the two hemes of cyt *b* (bc_1) in the mitochondrial membrane.

The asymmetric heme model

On the basis of EPR experiments on interactions of the low spin ferri-heme iron of the oxidized mitochondrial cyt *b* with external paramagnetic dysprosium (Dy^{3+}) complexes, the Fe^{2+} of heme b_n was inferred to be ~25 Å from both sides of the mitochondrial membrane (62). The thickness of the impermeable probe low polarity (ϵ_m) layer was assumed to be 50 Å, but is 40 Å if one takes into account the probe ion radius of 5 Å. The center of the b_n heme was situated on average at a distance of ~20 Å from both interfaces, but the b_p heme was localized just on the ϵ_m/ϵ_{in} boundary. Hence, an asymmetric disposition of cyt *b* in the membrane was implied,[4] which would make heme b_p protrude into the polar phase and cause a substantial decrease of the Bornian energy loss. Corresponding to this structure, the polar medium would also screen the field of the N termini of helices II and IV, and the total positive shift of the b_p potential would become much smaller.

To perform the calculations of the Bornian solvation energy for the heme ion crossing the boundary, formulae were derived on the basis of an approximation proposed by Kharkats and Ulstrup (Ref. 43; see Appendix, Fig. 6). Helices II and IV were assumed to protrude into the ϵ_{in} layer according to their link to heme b_p. Helices I and III were assumed to be fully immersed in the low-polarity region, with their COOH termini situated just at the interface and their axes parallel to and equidistant from helices II and IV. The alternative of helices I and III protruding into the intermediate-polarity region in the same way as helices II and IV seems less likely, because heme b_p would be surrounded by four hydrophobic helices, and hence it would not be in the higher polarity medium. The results of the calculations for the case of the center of the heme ion lying on the ϵ_m/ϵ_{in} boundary (Fig. 6 *C*) are presented in Table 3. A comparison with the "symmetric" model (Table 2) reveals the two largest effects that result from the positioning of heme

[4] Several indirect indications of a similar asymmetric structure were obtained on the basis of the influence of the *trans*-membrane potential on the heme E_m (63, 64) and carotenoid electrochromic shifts (65, 66). At the same time, an opposite asymmetric structure was inferred from experiments on heme accessibility to redox mediators (67).

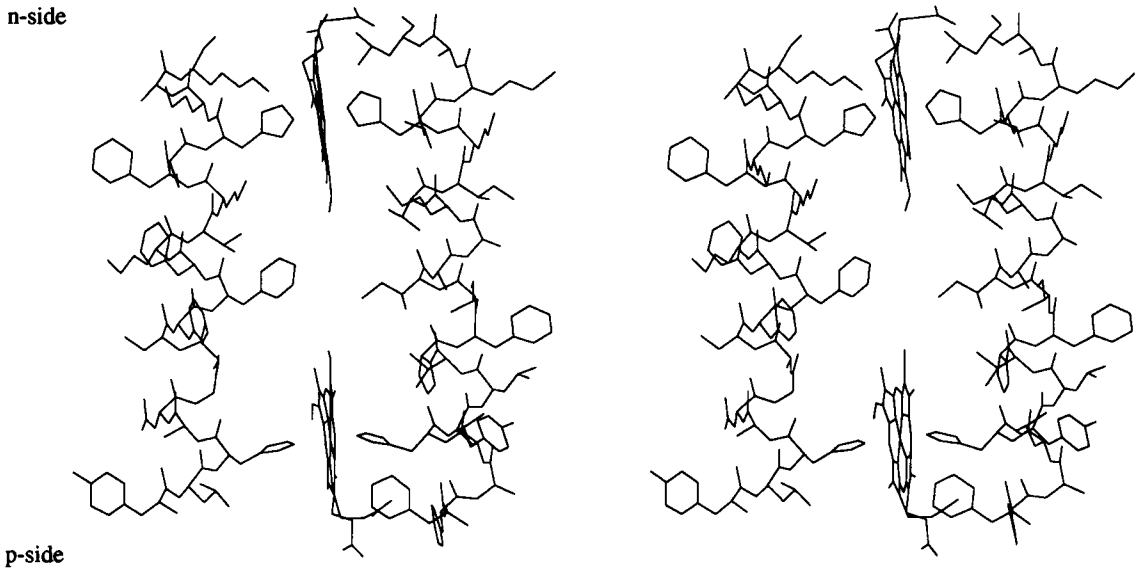

FIGURE 5 Molecular model (*stereo view*) of heme-bridged helices II (*left*) and IV (*right*) of yeast cyt *b* of the cytochrome bc_1 complex. The amino sequences of these two helices are: II, NH_2 (*p*-side)-YLHANGASFFFMVMFMHMA-COOH; IV, NH_2 (*p*-side)-FFALHYLVPFIIAAMVIMHLMAL-COOH. *n*- and *p*-sides (*top* and *bottom*, respectively).

b_p at the interface: (i) a decrease of the loss of solvation energy and (ii) a much stronger screening of the field of helices II and IV.

The results shown in Table 3 indicate that the predicted E_m of heme b_p is in better agreement with the experimental data. If the heme b_p center is displaced 1 Å into the ϵ_{in} and ϵ_m regions, the E_m will shift by +0.01 V or −0.01 V, respectively. Shifts of the COOH termini of helices I and III by 1 Å into the ϵ_{in} or ϵ_m layers would change the E_m by +0.02 V and −0.01 V. Although the agreement of the E_m value for heme b_n did not change very much in the *asymmetric* model, that for heme b_p decreased markedly and resulted in a ΔE_m with the correct sign, eliminating a qualitative contradiction inherent to the *symmetric* model. The dielectric asymmetry may arise from a higher polarity associated with the quinone binding niche of heme b_p (61).

DISCUSSION

Cytochrome b-559

In comparing redox potentials of a cofactor in solution and in membrane proteins, one has to take into account two major factors inherent to such proteins, the low dielectric constant of the membrane-protein medium and the permanent dipole electric field resulting from the long *trans*-membrane α-helices of integral membrane proteins. The low dielectric constant results in a loss of Bornian solvation energy that can increase the redox potential by as much as +0.2 V. The helix dipole field of two parallel helices can shift the potential positively or negatively by a similar value.

In the present paper, we have applied these concepts to an analysis of redox potentials of intramembraneous cytochromes *b*. The problem is of interest because (i) there has been no prior study of the dependence of the redox potential of the physiologically important membrane-bound *b* cytochromes on the electric field of the *trans*-membrane α-helices; (ii) a plausible physical-chemical explanation of the anomalously positive +0.4 V E_m value of cytochrome *b*-559 is important for the field of photosynthetic electron transport and bioenergetics.

The calculation of the effect of the electrostatic effects on the heme E_m values was carried out in the context of a three-layer dielectric model: ϵ_m = 3–4, 40 Å low polarity bilayer; ϵ_{in} = 12–20, 10–20 Å intermediate polarity surface layers, and ϵ_W = 80, bulk aqueous phase. The calculation of electrostatic effects based on a simple specific physical model allowed a fairly simple explanation of the unusually positive redox potential of cytochrome *b*-559. This evaluation took into account and supported the experimental conclusion (21) that the heme of this cytochrome is fully immersed in the low dielectric (ϵ_m) region of the membrane, but is situated close to its boundary with the region of intermediate dielectric (ϵ_{in}). A number of other smaller effects were discussed above that could alter the calculated E_m significantly if they were all operative. The net effect of all influences would be a positive shift in E_m that could move the calculated E_m even closer to the measured E_m of +0.40 V. Among the latter effects, it is worthwhile to consider the possible contribution to the E_m of structure changes in the protein itself. This was suggested by a shift in the g_z value of the low spin ferricytochrome *b*-559 EPR spectrum that correlated with transitions between the HP $\leftrightarrows$ LP cytochrome states. The g_z shift was attributed to a nonplanar arrangement of the two histidine ligands associated with the higher g_z = 3.08 value (3). An amide I-like differential signal detected by fourier transform infrared spectroscopy of the HP versus LP cytochrome *b*-559 led to the further suggestion that (i) the HP state is characterized by a hydrogen bond between a (-NH) of each histidine and a peptide bond carbonyl of each helix of the cytochrome. (ii) It was proposed that one of these bonds is removed in the LP state (68). The ΔE_m expected from this model is not known, although the extreme value of the ΔE_m (HP-LP) expected for orthogonal versus parallel histidine ring orientation, as mentioned above, is +0.05 V (47).

TABLE 2 Components of the midpoint redox potential of the hemes, b_n and b_p, of Cyt $b(bc_1)$ arranged symmetrically in the membrane bilayer

	Predicted potentials and potential changes (volts)		
	Heme b_n		Heme b_p
Potential in aqueous solution	−0.15		−0.15
Loss of the Bornian solvation energy	+0.18		+0.18
Shift of potential due to			
Field of helix II	−0.14[a]		+0.18[b]
Field of helix IV	−0.07[a]		+0.08[b]
Field of helices I and III	+0.12[b]		−0.10[a]
Value of midpoint redox potential, E_m	−0.06		+0.19
$\Delta E_m = E_m(b_p) - E_m(b_n)$		+0.25	
Experimental values	+0.05 to 0.09		−0.02 to −0.09
Experimental ΔE_m		−0.10 to −0.15	

[a] Effect due to potential at helix carboxyl terminus.

[b] Effect due to potential at helix amino terminus.

[c] The influence of variations of parameters like ϵ_{in} or δ_z for helix IV on the E_m values lies within the same limits as presented above for cyt *b*-559, the effect on the ΔE_m between b_n and b_p being practically negligible.

Cytochrome b (bc_1)

Reasonable models for the folding of the cytochrome polypeptide of the bc_1 and b_6f complex in the membrane have been described in the literature based mainly on the primary sequence and hydropathy/hydrophobicity analysis (54, 55, 60, 69) and molecular genetic analysis (56, 61, 70–73). Therefore, calculations have been carried out in the context of the proposed general structures. The calculations can be used as an additional tool for checking different hypotheses on the structure of these proteins.

The calculations for the model of two hemes of cyt *b* of the bc_1 complex arranged symmetrically in the membrane and fully immersed in its low-polar region resulted in a value for the ΔE_m between the two hemes that was incorrect in sign as well as magnitude, a qualitative contradiction with experiment. A model in which the center of heme b_p is close to the ϵ_m/ϵ_{in} boundary with a substantial part of this heme protruding into the region of higher polarity, and at the same time with heme b_n fully immersed in the inner part (ϵ_m) of the membrane, could be compatible with the experimental data for heme b_p. However, this model leads to a somewhat greater discrepancy with the measured values for the E_m of heme b_n. Therefore, a dielectric rather than geometric asymmetry, in which heme b_p is in contact with a local region of higher polarity, is necessary to provide a qualitatively correct description of the redox properties of hemes b_n and b_p.

Another reason for believing that the heme asymmetry is dielectric and not geometric is that a deep location of heme b_n in the nonpolar part (ϵ_m) of the thylakoid membrane seems unlikely for cyt b_6 of the b_6f complex because it was shown that the charged residues, Lys^{207} or even Arg^{206}, punctuating helix IV on the *n*-side of the membrane, are accessible to trypsin in situ (74). This is consistent with the His^{201} heme ligand of heme b_n of the cyt b_6 occupying approximately the same position as in the "symmetric" model. The large distance (20 Å) of heme b_n from the surface observed in mitochondrial membranes by Ohnishi et al. (62) may not be present in the cyt b_6f complex that has a much simpler polypeptide subunit composition. It is also possible that the asymmetry of the mitochondrial cyt *b* inferred from the EPR studies with the dysprosium complex could have been the result of a surface protein barrier to the probe.

APPENDIX

The electrostatic problem for the case of a charged sphere crossing the planar boundary between two dielectrics has no explicit analytical solution. A reasonable approximation for this problem was proposed by Kharkats and Ulstrup (43) who have taken the field of the point charge in the system with a single planar interface and then integrated it over all the surfaces including the spherical one. This approximation smoothly connects the strict solution when the center of a spherical ion of radius a moves from the boundary to the distance h>a. Their result for the energy of the system has the form

$$W_{KU} = \frac{(ze)^2}{4a}\left\{\frac{1}{\epsilon_1}(1+y) + \frac{1}{\epsilon_2}\left(\frac{2\epsilon_2}{\epsilon_1+\epsilon_2}\right)^2(1-y) + \frac{\epsilon_1-\epsilon_2}{\epsilon_1+\epsilon_2}(2-y) + \frac{1}{2\epsilon_1}\left(\frac{\epsilon_1-\epsilon_2}{\epsilon_1+\epsilon_2}\right)^2\left[\frac{(1+y)(1-2y)}{1+2y} + \frac{1}{2y}\ln(1+2y)\right]\right\} \quad \text{(A1)}$$

where ze is the charge of the ion, ϵ_1, and ϵ_2 the dielectric constants, respectively, of the medium where the center of the ion is situated, and of the other medium, and $y = h/a$ (Fig. 6).

Using the same approximation, we have considered the problem of a system having an additional interlayer with the center of the ion situated in the low-polarity phase (Fig. 6 *A*) or in the layer of intermediate polarity (Fig. 6 *B*). This system is a valid description for the membrane model used throughout this paper because in the case of an ion crossing one membrane surface the opposite surface is far enough away (40 Å) that its effect can be ignored. The electrostatic free energy can be found by integration of the product of displacement and electric field vectors over the whole space of the system. The problem may be handled more conveniently by conversion of spatial integrals into surface ones. In that case, the integrals over planar surfaces cancel each other and only the integrals over the sphere remain (see, e.g., Ref. 43). The surface integrals have the form $\int d\mathbf{s}\cdot\varphi\,\nabla\varphi$, where $d\mathbf{s}$ is the external vector of a surface element normal to the surface, and φ and $-\varphi$ are the electric potential and its gradient. For the point charge and one of its images, φ consists of two corresponding contributions, φ_c and φ_{im}. In

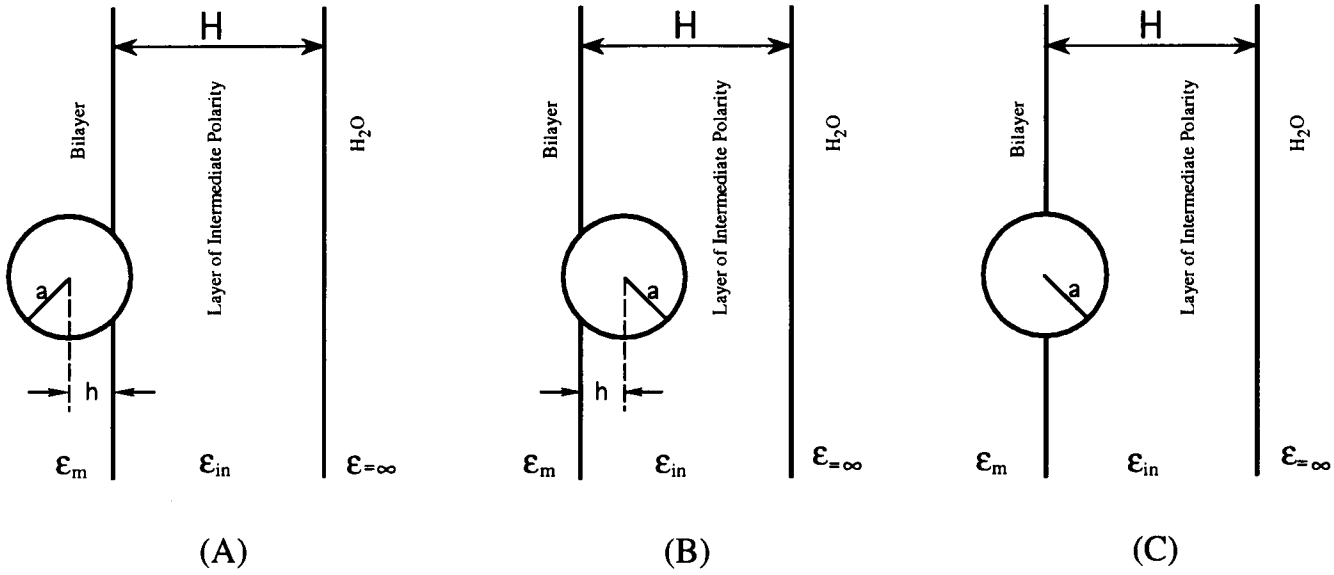

FIGURE 6 Scheme for heme ion crossing the ϵ_m/ϵ_{in} boundary. Ion center in (*A*) the membrane bilayer (dielectric constant, ϵ_m), (*B*) in the surface layer of intermediate dielectric constant (ϵ_{in}), and (*C*) at the ϵ_m/ϵ_{in} boundary.

TABLE 3 Components of the redox potential of Cyt $b(bc_1)$ arranged asymmetrically in the membrane with heme b_p positioned at the ϵ_m–ϵ_{in} boundary

	Potentials and potential changes (volts)		
	Heme b_n		Heme b_p
Potential in aqueous solution	−0.15		−0.15
Loss of Bornian solvation energy	+0.22		+0.04
Shift of potential due to			
Field of helix II	−0.16[a]		+0.06[c]
Field of helix IV	−0.15[a]		+0.02[c]
Field of helices I and III[b]	+0.15[c]		
Value of midpoint redox potential, E_m	−0.09		−0.12
$\Delta E_m = E_m(b_p) - E_m(b_n)$		−0.03	
Experimental values	+0.05 to +0.09		−0.02 to −0.09
Experimental ΔE_m		−0.10 to −0.15	

[a] Effect due to potential at helix carboxyl terminus.
[b] Calculated with $\epsilon_{in} = 20$.
[c] Effect due to potential at helix amino terminus.

the surface integral, the terms for four types are obtained: $\varphi_c \nabla\varphi_c$, $\varphi_{im} \nabla\varphi_c$, $\varphi_c \nabla\varphi_{im}$, and $\varphi_{im} \nabla\varphi_{im}$.

The first of these terms gives the value of usual charging energy of Bornian type, which equals $(ze)^2/2\epsilon a$ in a homogeneous medium. This Bornian energy in our system is described by the first two terms in Eq. A1 corresponding to two dielectric media bordering the ion. Note that for a homogeneous medium, i.e., $\epsilon_1 = \epsilon_2$, Eq. A1 transforms to the Bornian expression.

The second type of surface integral gives the energy of interaction of the point charge with its image, and equals $ze\varphi_{im}/2$ in the case of $h > a$. In the case of a sphere fully immersed in one dielectric, the third integral becomes zero, because the flux of a gradient through a closed surface is zero. In the present case, there are two unclosed surfaces in two different media, and the integral does not vanish. It gives a correction to the charge-image interaction. The sum of the second and third integrals gives the third term in Eq. A1. The last integral provides a correction for the finite size of the ion. Its value is given in the last two terms of Eq. A1.

In the present problem, in the system with an interlayer, the total field includes the fields of several additional series of images, and one must add to the energy W_{KU} the energies of interaction of the charge with additional images (integrals of the second and third types). The finite size correction decays rapidly with increasing distance, and hence we have neglected these terms for all images except the first one included in W_{KU}. The calculation is facilitated by the largest of the small correction terms for subsequent images having opposite signs and almost canceling. The results are as follows.

For the case of the ion center situated in the low-polarity phase with dielectric constant ϵ_m (Fig. 6 *A*).

$$W = W_{KU} - \frac{4(Ze)^2\epsilon_m}{(\epsilon_{in} + \epsilon_m)^2} \times \sum_0^\infty E^n[\alpha(2nH + 2H + 2ay) + \mu(2nH + 2H + 2ay)] - \frac{2(Ze)^2}{\epsilon_{in} + \epsilon_m} \times \sum_0^\infty \{E^n[\gamma(2nH + 2H + 2ay) + \xi(2nH + 2H + 2ay)] - E^{n+1}[\beta(2nH + 2H) + \nu(2nH + 2H)]\} \quad \text{(A2)}$$

For the ion center in the layer of intermediate dielectric constant ϵ_{in} (Fig. 6 *B*):

$$W = W_{KU} + \frac{1(Ze)^2}{\epsilon_{in}} \sum_0^\infty \{ -E^n[\delta(2nH + 2H - 2ay) + \chi(2nH + 2H - 2ay)] + E^{n+1}[\alpha(2nH + 2H) + \delta(2nH + 2H) + \mu(2nH + 2H) + \chi(2nH + 2H)]\} - E^{n+2}[\alpha(2nH + 2H + 2ay) + \mu(2nH + 2H + 2ay)]\} + \frac{2(Ze)^2}{\epsilon_{in} + \epsilon_m} \times \sum_0^\infty -E^n[\beta(2nH + 2H - 2ay) + \nu(2nH + 2H - 2ay)] + E^{n+1}[\beta(2nH + 2H) + \nu(2nH + 2H)]\} \quad (A3)$$

Here the Greek letters are used to designate the integrals obtained in different limits as a function of the charge-image distance l and the parameter y:

$$\alpha(l, y) = \frac{1}{4al}(A - L); \qquad \beta(l, y) = \frac{1}{4al}(A - K) \quad (A4)$$

$$\gamma(l, y) = \frac{1}{4al}(L - B); \qquad \delta(l, y) = \frac{1}{4al}(K - B) \quad (A5)$$

$$\mu(l, y) = \frac{a}{4}\left[-\frac{1}{A}(1/a + 1/l) + \frac{1}{L}(1/l - y/a) + \frac{1}{a^2 l}(A - L)\right] \quad (A6)$$

$$\nu(l, y) = \frac{a}{4}\left[-\frac{1}{A}(1/a + 1/l) + \frac{1}{K}(1/l + y/a) + \frac{1}{a^2 l}(A - K)\right] \quad (A7)$$

$$\chi(l, y) = \frac{a}{4}\left[\frac{1}{B}(-1/a + 1/l) - \frac{1}{K}(1/l + y/a) + \frac{1}{a^2 l}(K - B)\right] \quad (A8)$$

$$\xi(l, y) = \frac{a}{4}\left[\frac{1}{B}(1/l - 1/a) - \frac{1}{L}(1/l - y/a) + \frac{1}{a^2 l}(L - B)\right] \quad (A9)$$

with designations

$$A = l + a; \quad B = l - a; \quad K = (l^2 + a^2 + 2aly)^{1/2};$$
$$L = (l^2 + a^2 - 2aly)^{1/2}; \quad E = (\epsilon_{in} - \epsilon_m)/(\epsilon_{in} + \epsilon_m) \quad (A10)$$

In the case $y = 0$ (Fig. 6 *C*), i.e., the center of the ion being exactly on the boundary, $W_{KU} = (ze)^2/a\ (\epsilon_{in} + \epsilon_m)$, which is the Bornian charging energy at the effective $\epsilon = (\epsilon_{in} + \epsilon_m)/2$ (see Ref. 43). It can be shown that at $y = 0$, Eqs. A2 and A3 coincide.

We thank C. V. Stauffacher and P. Elkins for discussions on the graphics analysis, Y. Kharkats and J. Ulstrup for helpful discussion, Janet Hollister for reducing the chaos of this manuscript to order, and Profs. V. E. Kazarinov and K. L. Kliewer for facilitating the cooperation of the authors through the exchange agreement.

This research was supported by grant GM-38326 from the National Institutes of Health (WAC), and an exchange agreement between the Frumkin Institute of Electrochemistry and the Purdue University School of Science.

REFERENCES

1. Falk, J. E. 1964. Porphyrins and Metalloporphyrins. Elsevier, Amsterdam. 235–300.
2. Kassner, R. J. 1972. Effects of nonpolar environments on the redox potentials of heme complexes. *Proc. Natl. Acad. Sci. USA.* 69:2263–2267.
3. Babcock, G. T., W. R. Widger, W. A. Cramer, W. A. Oertling, and J. G. Metz. 1985. Axial ligands of chloroplast cytochrome *b*-559: identification and requirement for a heme-cross-linked polypeptide structure. *Biochemistry* 24:3638–3645.
4. Moore, G. R., G. W. Pettigrew, and N. K. Rogers. 1986. Factors influencing redox potentials in electron transfer proteins. *Proc. Natl. Acad. Sci. USA.* 83:4998–4999.
5. Krishtalik, L. I. 1986. Charge Transfer Reactions in Electrochemical and Chemical Processes. Plenum Press, New York. Chap. 7.
6. Gunner, M. R., and Honig, B. 1991. Electrostatic control of midpoint potentials in the cytochrome subunit of the *Rps. sphaeroides* reaction center. *Proc. Natl. Acad. Sci. USA.* 88:9151–9155.
7. Cramer, W. A., and D. B. Knaff. 1991. Energy Transduction in Biological Membranes. Chap. 2 and 7. Springer-Verlag, New York. 579 pp.
8. Deisenhofer, J., and H. Michel. 1989. The photosynthetic reaction center from the purple bacterium *Rhodopseudomonas viridis*. *EMBO J.* 8:2149–2169.
9. Warshel, A., and S. T. Russel. 1984. Calculation of electrostatic interactions in biological systems and in solutions. *Quart. Rev. Biophys.* 17:283–422.
10. Rogers, N. K. 1986. The modeling of electrostatic interactions in the function of globular proteins. *Prog. Biophys. Mol. Biol.* 48:37–66.
11. Honig, B. H., W. L. Hubbell, and R. F. Flewelling. 1986. Electrostatic interactions in membranes and proteins. *Ann. Rev. Biophys. Biophys. Chem.* 15:163–194.
12. Krishtalik, L. I. 1985. Effective activation energy of enzymatic and nonenzymatic reactions. Evolution-imposed requirements on enzyme structure. *J. Theor. Biol.* 112:251–264.
13. Krishtalik, L. I. 1988. Charge-medium interactions in biological charge-transfer reactions. *In* The Chemical Physics of Solvation. R. R. Dogonadze, E. Kálmán, A. A. Kornyshev, and J. Ulstrup, editors. Elsevier Science Publishers, Amsterdam. Part C:707–740.
14. Sharp, K. A., and Honig, B. 1990. Electrostatic interactions in macromolecules: theory and applications. *Annu. Rev. Biophys. Biophys. Chem.* 19:301–332.
15. Warshel, A., and J. Åquist. 1991. Electrostatic energy and macromolecular function. *Annu. Rev. Biophys. Biophys. Chem.* 20:267–298.
16. Sheridan, R. P., and L. C. Allen. 1980. The electrostatic potential of the alpha helix (Electrostatic potential/α-helix/secondary structure/helix dipole). *Biophys. Chem.* 11:133–136.
17. Hol, W. G. J. 1985. The role of the α-helix dipole in protein function and structure. *Prog. Biophys. Mol. Biol.* 45:149–195.
18. Kyte, J., and R. F. Doolittle. 1982. A simple method for displaying the hydrophathic character of a protein. *J. Mol. Biol.* 157:105–132.
19. Cramer, W. A., S. M. Theg, and W. R. Widger. 1986. On the structure and function of cytochrome *b*-559. *Photosyn. Res.* 10:393–403.
20. Widger, W. R., and W. A. Cramer. 1991. The cytochrome b_6f complex. *In* Cell Culture and Somatic Cell Genetics of Plants: The Molecular Biology of Plastids and the Photosynthetic Apparatus. I. K. Vasil and L. Bogorad, editors. Academic Press, Orlando. 149–176.
21. Tae, G.-S., M. T. Black, W. A. Cramer, O. Vallon, and L. Bogorad. 1988. Thylakoid membrane protein topography: transmembrane orientation of the chloroplast cytochrome *b*-559 *psb*E gene product. *Biochemistry.* 27:9075–9080.
22. Horton, P., J. Whitmarsh, and W. A. Cramer. 1976. On the specific site of action of 3-(3,4-dichlorophenyl)-1,1-dimethylurea in chloroplasts: inhibition of a dark acid-induced decrease in midpoint potential of cytochrome *b*-559. *Arch. Biochem. Biophys.* 176:519–524.
23. Whitmarsh, J., and W. A. Cramer. 1977. Kinetics of the photoreduction of cytochrome *b*-559 by photosystem II in chloroplasts. *Biochim. Biophys. Acta. 460*:280–289.
24. Neumcke, B., and P. Läuger. 1969. Nonlinear electrical effects in lipid bilayer membranes: II. Integration of the generalized Nernst-Planck equations. *Biophys. J.* 9:1160–1170.
25. Krishtalik, L. I. 1986. Activation energy for charge transfer reactions in membranes. Proton-translocating proteins. *J. Electroanal. Chem.* 204:245–255.
26. Cherepanov, D. A., and L. I. Krishtalik. 1990. Intramembrane electric

fields: a single charge, protein α-helix, photosynthetic reaction center. *Bioelectrochem. Bioenerg.* 24:113–127.

27. Gennis, R. B. 1989. Biomembranes: Molecular Structure and Function. Springer Verlag, New York. Chap. 1.
28. Aytian, S. K., S. S. Dukhin, and Y. A. Chizmadzhev. 1977. Image force effects on charge movements in membranes. *Elektrokhimiya.* 13:779–783.
29. Lelkes, P. I., and I. R. Miller. 1980. Perturbations of membrane structure by optical probes: I. Location and structural sensitivity of merocyanine 540 bound to phospholipid membranes. *J. Membr. Biol.* 52:1–15.
30. Cevc, G., A. Watts, and D. Marsh. 1981. Titration of the phase transition of phosphatidylserine bilayer membranes. Effects of pH, surface electrostatics, ion binding, and head-group hydration. *Biochemistry.* 20: 4955–4965.
31. Ashkroft, R. G., H. G. L. Coster, D. R. Laver, and J. R. Smith. 1983. The effects of cholesterol inclusion on the molecular organisation of bimolecular lipid membranes. *Biochim. Biophys. Acta.* 730:231–238.
32. Pethig, R. 1979. Dielectric and Electronic Properties of Biological Materials. Wiley, New York. 376 pp.
33. Wada, A. 1976. The α-helix as an electric macro-dipole. *In* Adv. Biophys. M. Kotani, editor. University of Tokyo Press, Tokyo, University Park Press, Baltimore, London, and Tokyo. 9:1–63.
34. Krishtalik, L. I., and V. V. Topolev. 1983. The intraglobular electric field of an enzyme. I. The primary field set up by the polypeptide backbone, functional groups and ions of the α-chymotrypsin molecule. *Molekul. Biologiya* 17:1034–1041.
35. Van Duijnen, P. T., and B. T. Thole. 1982. Cooperative effects in α-helices: an *ab initio* molecular-orbital study. *Biopolymers* 21:1749–1761.
36. Alpatova, N. M., E. V. Ovsyannikova, and L. I. Krishtalik. 1991. A study of redox reactions of cobalticenium and ruthenium-bipyridyl complex with the aim of comparison of cation and anion solvation in aprotic and protic media. *Elektrokhimiya.* 27:931–933.
37. Krishtalik, L. I., N. M. Alpatova, and E. V. Ovsyannikova. 1991. Electrostatic ion-solvent interaction. *Electrochim. Acta.* 36:435–445.
38. Mathews, F. S., and E. W. Czerwinski. 1985. Cytochrome b_5 and cytochrome b_5 reductase from a chemical and X-ray diffraction viewpoint. *In* The Enzymes of Biological Membranes. Vol. 4. 2nd ed. A. Martonosi, editor. Plenum, New York. 235–300.
39. Falk, J. E., and D. D. Perrin. 1961. Spectra and redox potential of metalloporphyrins and haemoproteins. *In* Haematin Enzymes. J. E. Falk, R. Lemberg, and R. K. Morton, editors. Pergamon, Oxford. I:56–71.
40. Warme, P. K., and L. P. Hager. 1970. Heme sulfuric anhydrides. II. Properties of heme models prepared from mesoheme sulfuric anhydrides. *Biochemistry.* 9:1606–1614.
41. Barron, E. S. G. 1937. Studies on biological oxidations. IX. The oxidation-reduction potentials of blood hemin and its hemochromogens. *J. Biol. Chem.* 121:285–312.
42. Yerkes, C. T., and A. R. Crofts. 1984. A mechanism for ADRY-induced photooxidation of cytochrome *b*-559. *In* Adv. Photosyn. Res. C. Sybesma, editor. M. Nijhoff, The Hague. I:489–492.
43. Kharkats, Y. I., and J. Ulstrup. 1991. The electrostatic free energy of finite-size ions near a planar boundary between two dielectric media. *J. Electroanalyt. Chem.* 308:17–26.
44. Moore, G. 1983. Control of redox properties of cytochrome *c* by special electrostatic interactions. *FEBS Lett.* 161:171–175.
45. Reid, L. S., M. R. Mauk, and A. G. Mauk. 1984. Role of heme propionate groups in cytochrome b_5 electron transfer. *J. Am. Chem. Soc.* 106:2182–2185.
46. Rogers, N. K., C. R. Moore, and M. J. E. Sternberg. 1985. Electrostatic interactions in globular proteins: calculation of the pH dependence of the redox potential of cytochrome c_{551}. *J. Mol. Biol.* 182:613–616.
47. Walker, F. A., B. H. Huynh, W. R. Scheidt, and S. R. Oswath. 1986. Models of the cytochromes *b*. Effect of axial ligand plane orientation on the EPR and Mössbauer spectra of low-spin ferrihemes. *J. Am. Chem. Soc.* 108:5288–5297.
48. Cramer, W. A., and J. Whitmarsh. 1977. Photosynthetic cytochromes. *Ann. Rev. Pl. Physiol.* 28:133–172.
49. Song-Xiao, K. Fushimi, and K. Satoh. 1990. The D1–D2 complex of the photosystem II complex from spinach. *FEBS Lett.* 273:257–260.
50. Cramer, W. A., J. Whitmarsh, and W. Widger. 1981. On the properties and function of cytochrome *b*-559 and *f* in chloroplast electron transport. *In* Photosynthesis: Electron Transport and Phosphorylation. G. Akoyunoglou, editor. Balaban International Science Services, Philadelphia. 509–522.
51. Fan, H. N., and W. A. Cramer. 1970. The redox potential of cytochrome *b*-559 and *b*-563 in spinach chloroplasts. *Biochim. Biophys. Acta.* 216: 200–207.
52. Cramer, W. A., J. Whitmarsh, and P. S. Low. 1981. Differential scanning calorimetry of chloroplast membranes: identification of an endothermic transition associated with the water-splitting complex of photosystem II. *Biochemistry.* 20:157–162.
53. Nobrega, F. G., and A. Tzagoloff. 1980. Analysis of the mitochondrial membrane system. DNA sequence and organization of the cytochrome *b* gene in *S. cerevisiae*. *J. Biol. Chem.* 255:9828–9837.
54. Widger, W. R., W. A. Cramer, R. Herrmann, and A. Trebst. 1984. Sequence homology and structural similarity between cytochrome *b* of mitochondrial complex III and the chloroplast b_6-*f* complex: position of the cytochrome *b* hemes in the membrane. *Proc. Natl. Acad. Sci. U.S.A.* 81:674–678.
55. Saraste, M. 1984. Location of haem-binding sites in the mitochondrial cytochrome *b*. *FEBS Lett.* 166:367–372.
56. di Rago, J.-P., P. Netter, and P. P. Slonimski, 1990. Intragenic suppressors reveal long distance interactions between inactivating and reactivating amino acid replacements generating three-dimensional constraints in the structure of mitochondrial cytochrome *b*. *J. Biol. Chem.* 265:15750–15757.
57. Crofts, A. R. 1985. The mechanism of the ubiquinol:cytochrome *c* oxidoreductases of mitochondria and of *Rhodopseudomonas sphaeroides*. *In* The Enzymes of Biological Membranes. A. Martonosi, editor. Plenum, New York. 347–382.
58. Rich, P. R., A. E. Jeal, S. A. Madgwick, and A. J. Moody. 1990. Inhibitor effects on redox-linked protonations of the *b* haems of the mitochondrial bc_1 complex. *Biochim. Biophys. Acta.* 1018:29–40.
59. Crofts, A. R., H. Robinson, K. Andrews, S. van Doren, and E. Berry. 1987. Catalytic sites for reduction and oxidation of quinones. *In* Cytochrome Systems: Molecular Biology and Bioenergetics. S. Papa, B. Chance, and L. Ernster, editors. Plenum Press, New York. 617–624.
60. Brasseur, R. 1988. Calculation of the three-dimensional structure of *S. cerevisiae* cytochrome *b* inserted into a lipid matrix. *J. Biol. Chem.* 263:12571–12575.
61. Robertson, D. E., F. Daldal, and P. L. Dutton. 1990. Mutants of ubiquinol-cytochrome c_2 oxidoreductase resistant to Q_o site inhibitors: Consequences for ubiquinone and ubiquinol affinity and catalysis. *Biochemistry* 29:11249–11260.
62. Ohnishi, T., H. Schagger, S. W. Meinhardt, R. LoBrutto, T. A. Link, and G. von Jagow. 1989. Spatial organization of the redox active centers in the bovine heart ubiquinol-cytochrome *c* oxidoreductase. *J. Biol. Chem.* 264:735–744.
63. Konstantinov, A. A., W. S. Kung, and Y. A. Kamensky. 1981. The Q cycle in the mitochondrial respiratory chain. *In* Chemiosmotic Proton Circuits in Biological Membranes. V. P. Skulachev and P. C. Hinkle, editors. Addison-Wesley Publ. Co., Reading, PA. 123–146.
64. Gopher, A., and M. Gutman. 1982. Differentiation between c and m side reactions of ubiquinone using an imposed electrochemical potential gradient. *In* Function of Quinones in Energy Conserving Systems. B. L. Trumpower, editor. Academic Press, New York. 511–546.
65. Glaser, E. A., and A. R. Crofts. 1984. A new electrogenic step in the ubiquinol:cytochrome c_2 oxidoreductase complex of *Rhodopseudomonas sphaeroides*. *Biochim. Biophys. Acta.* 766:322–333.
66. Robertson, D. E., and P. L. Dutton. 1988. The nature and magnitude of the charge-separation reactions of ubiquinol:cytochrome c_2 oxidoreductase. *Biochim. Biophys. Acta.* 935:273–291.
67. Konstantinov, A. A., and E. Popova. 1987. Topography and protonmotive mechanism of mitochondrial coupling site 2. *In* Cytochromes: Molecular Biology and Bioenergetics. S. Papa, B. Chance, and L. Ernster, editors. Plenum Publ. Co., New York. 751–765.
68. Berthomieu, C., A. Boussac, W. Mäntele, J. Breton, and E. Nabedryk. 1992. Molecular changes following oxidoreduction of cytochrome *b*-559 characterized by Fourier transform infrared spectroscopy: photooxidation in photosystem II and electrochemistry of protoporphyrin IX-bis imidazole model compounds. *Biochemistry.* 31:11460–11471.

69. Degli Esposti, M. 1989. Prediction and comparison of the haem-binding sites in membrane haemoproteins. *Biochim. Biophys. Acta.* 977:249–285.

70. di Rago, J.-P., and A.-M. Colson. 1988. Molecular basis for resistance to antimycin and diuron, Q-cycle inhibitors acting at the Q_i site in the mitochondrial ubiquinol-cytochrome *c* reductase in *Saccharomyces cerevisiae*. *J. Biol. Chem.* 263:12564–12570.

71. di Rago, J.-P., J.-Y. Coppeé, and A.-M. Colson. 1989. Molecular basis for resistance to myxothiazol, mucidin (strobilurin A), and stigmatellin. *J. Biol. Chem.* 264:14543–14548.

72. Yun, C.-H., A. R. Crofts, and R. B. Gennis. 1991. Assignment of the histidine axial ligands to the cytochrome b_H and cytochrome b_L components of the bc_1 from *Rhodobacter sphaeroides* by site-directed mutagenesis. *Biochemistry.* 30:6747–6754.

73. Yun, C.-H., S. R. van Doren, A. R. Crofts, and R. B. Gennis. 1991. The use of gene fusions to examine the membrane topology of the L-subunit of photosynthetic reaction center and of the cytochrome *b* subunit of the bc_1 complex from *Rhodobacter sphaeroides*. *J. Biol. Chem.* 266:10967–10973.

74. Szczepaniak, A., and W. A. Cramer. 1990. Thylakoid membrane protein topography: location of the termini of the chloroplast cytochrome b_6 on the stromal side of the membrane. *J. Biol. Chem.* 265:17720–17726.